Electronic Supplementary Material (ESI) for Journal of Materials Chemistry B.

Active-targeting and acid-sensitive pluronic prodrug micelles for efficiently overcoming MDR in breast cancer

Xu Cheng, Jiaxi Xu, Yan Zheng, Qin Fang, Xiaodong Lv, Xin Wang, Rupei Tang*

Engineering Research Center for Biomedical Materials, Anhui Key Laboratory of Modern Biomanufacturing, School of Life Sciences, Anhui University, 111 Jiulong Road, Hefei, Anhui Province, 230601, P. R. China

* Corresponding author.

Email: tangrp99@iccas.ac.cn (R. Tang)

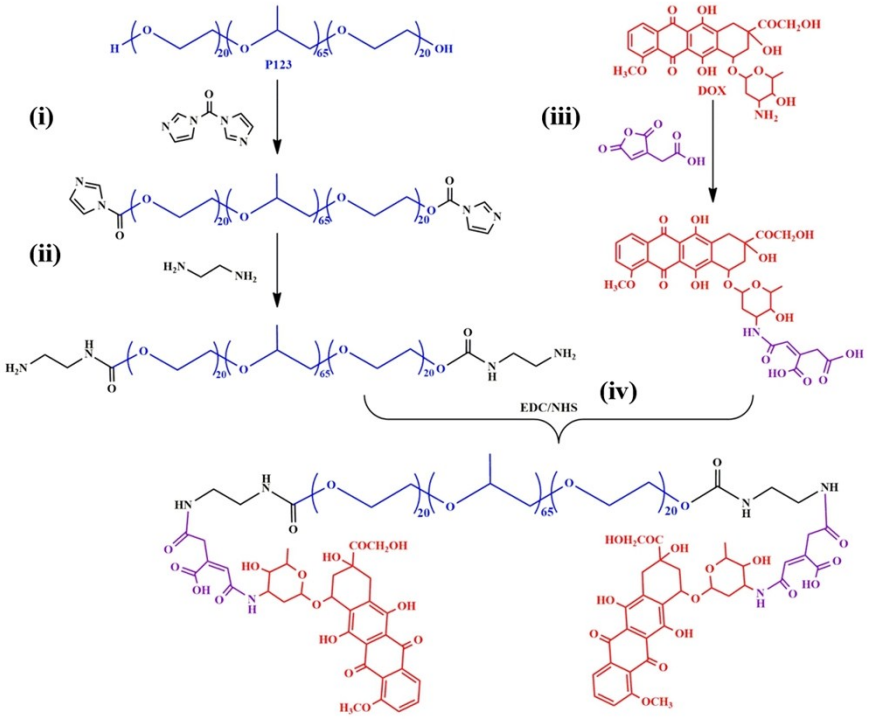

Fig. S1. Synthetic route of pluronic copolymer prodrug (P123-CAD); Reaction conditions: (i) anhydrous dichloromethane; (ii) anhydrous dimethyl sulfoxide; (iii) 0.1 M PB solution, pH 8.0, 0℃; (4) EDC/NHS, TEA, 25℃.

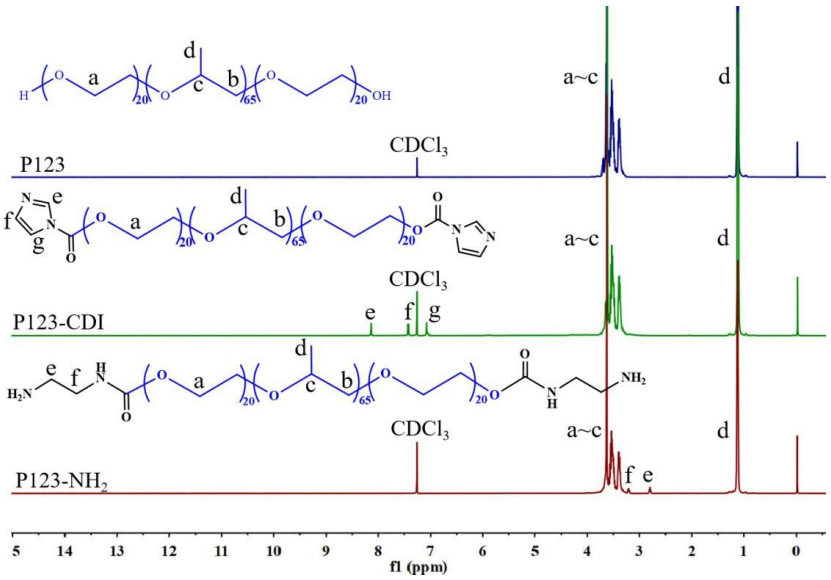

Fig. S2. ^{1}H NMR spectra of P123, P123-CDI and P123-NH_2, and $CDCl_3$ was used as the solvent.

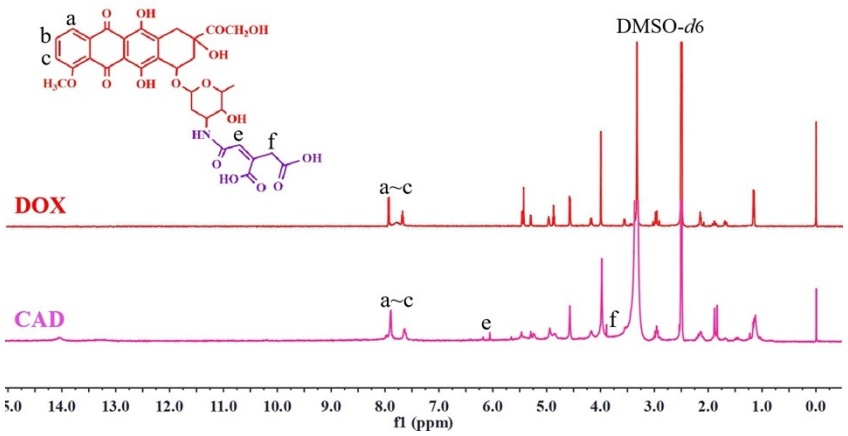

Fig. S3. ^{1}H NMR spectra of DOX and CAD, and DMSO-$_{d6}$ was used as the solvent.

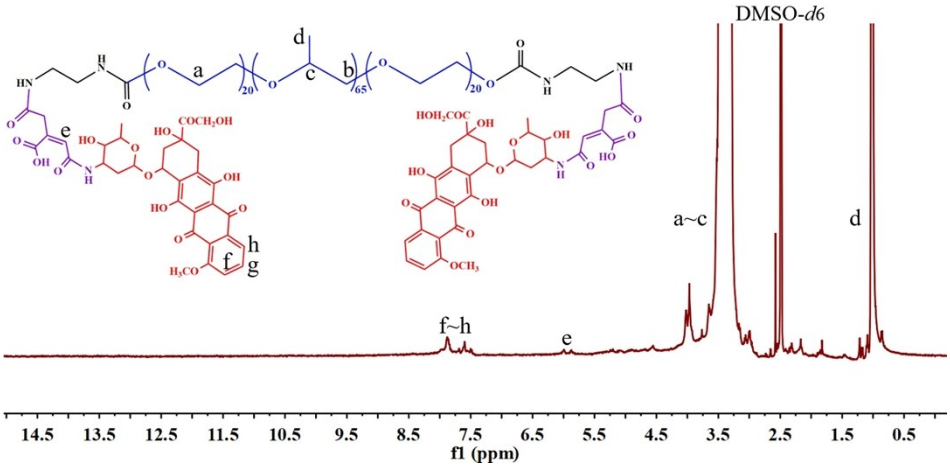

Fig. S4. ^{1}H NMR spectra of pluronic copolymer prodrugs (P123-CAD), and DMSO-$_{d6}$ was used as the solvent.

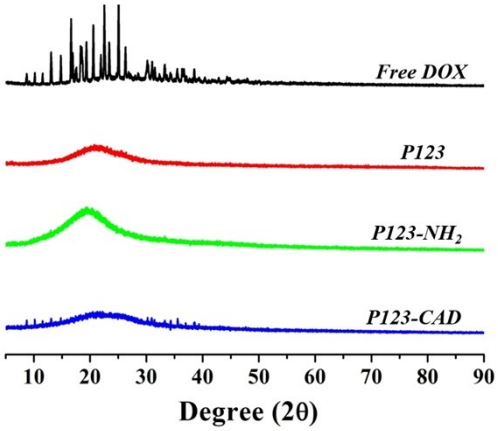

Fig. S5. XRD pattern of free DOX, P123, P123-NH_2 and P123-CAD.

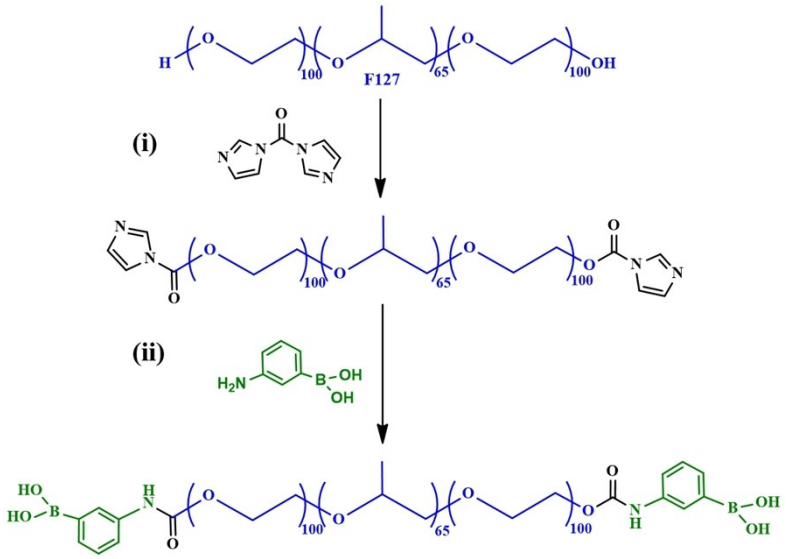

Fig. S6. Synthetic route of active-targeting pluronic copolymer (F127-PBA); Reaction conditions: (i) anhydrous dichloromethane; (ii) dimethyl sulfoxide, 0.2% DMAP, at room temperature for 48 h.

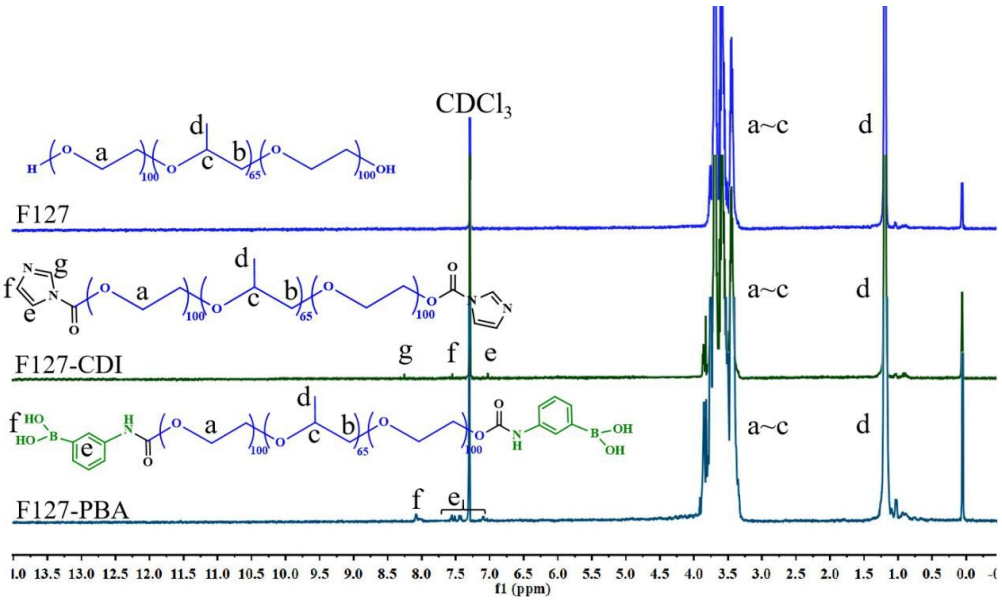

Fig. S7. ^{1}H NMR spectra of F127, F127-CDI and F127-PBA, and $CDCl_3$ was used as the solvent.

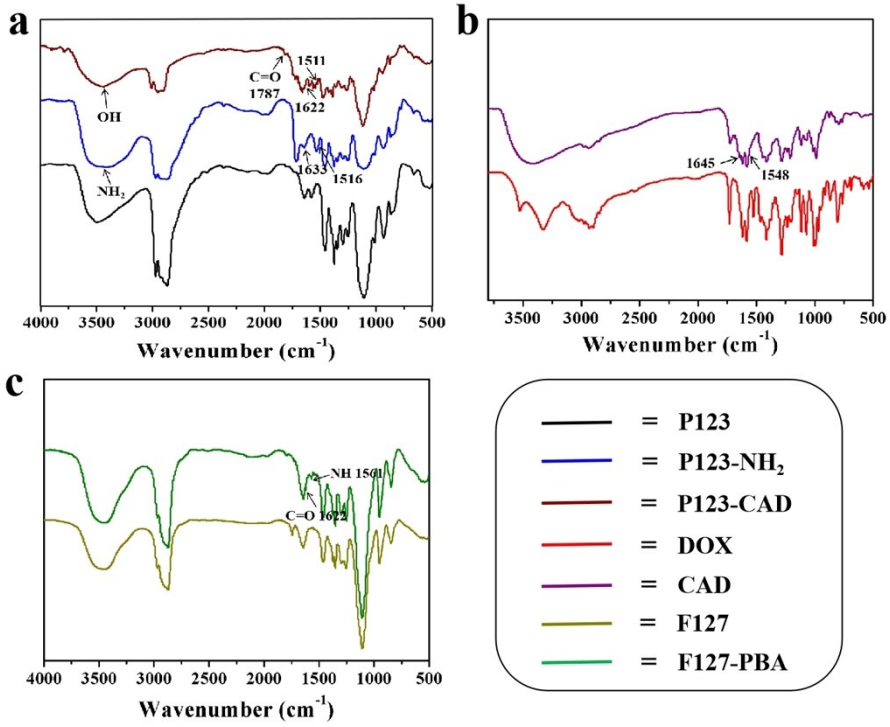

Fig. S8. FT-IR spectra of (a) P123, P123-NH_2 and P123-CAD; (b) DOX and CAD; (c) F127 and F127-PBA.

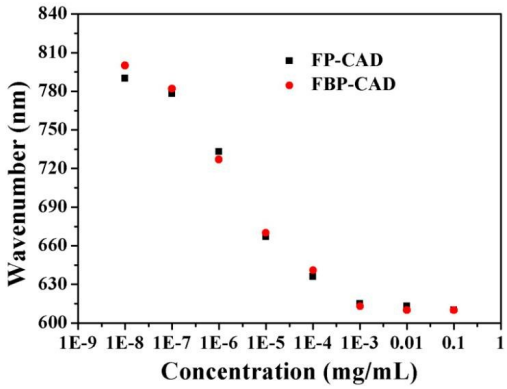

Fig. S9. The CMC value of FP-CAD and FBP-CAD.

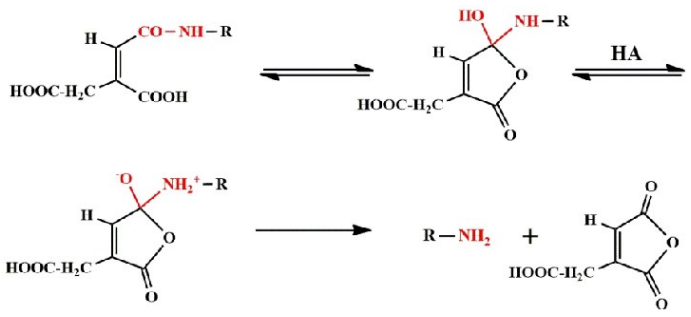

Fig. S10. The degradation mechanism of CAD in acid conditions.

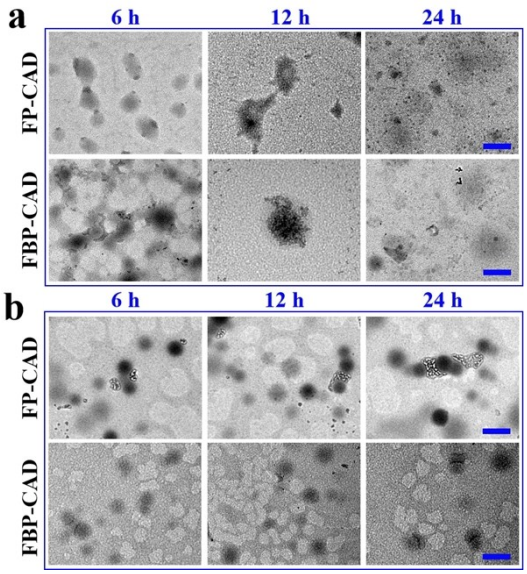

Fig. S11. Morphology change of prodrugs particles in pH 5.0 (a) and pH 7.4 (b), scale bar = 200 nm.

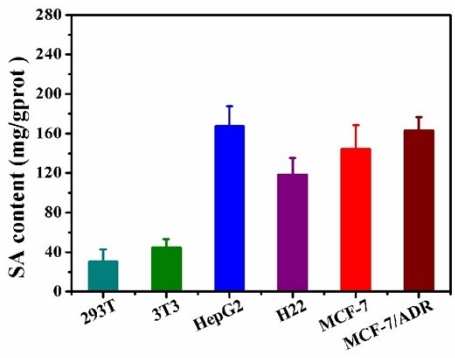

Fig. S12. Sialic acid (SA) content in different types of cells.

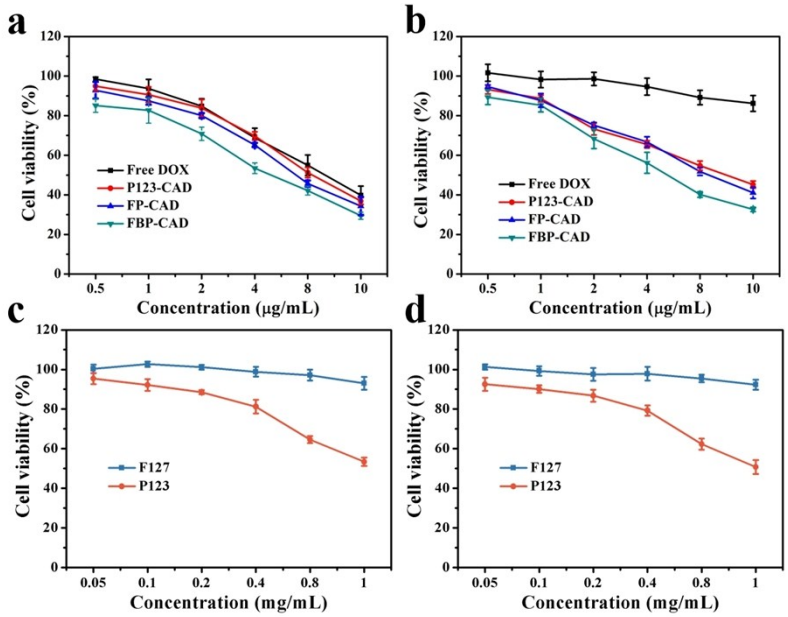

Fig. S13. MTT method evaluated the cytotoxicity of four DOX formulations in MCF-7 cells (a) and MCF-7/ADR cells (b); Anti-proliferation ability of pluronic copolymer in MCF-7 cells (c) and MCF-7/ADR cells (d); Data are represented as mean ± SD (n = 6).

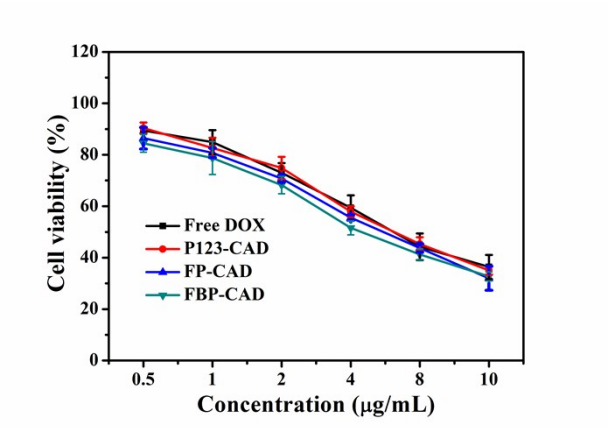

Fig. S14. In vitro cytotoxicity of different DOX formulations in 3T3 cells.

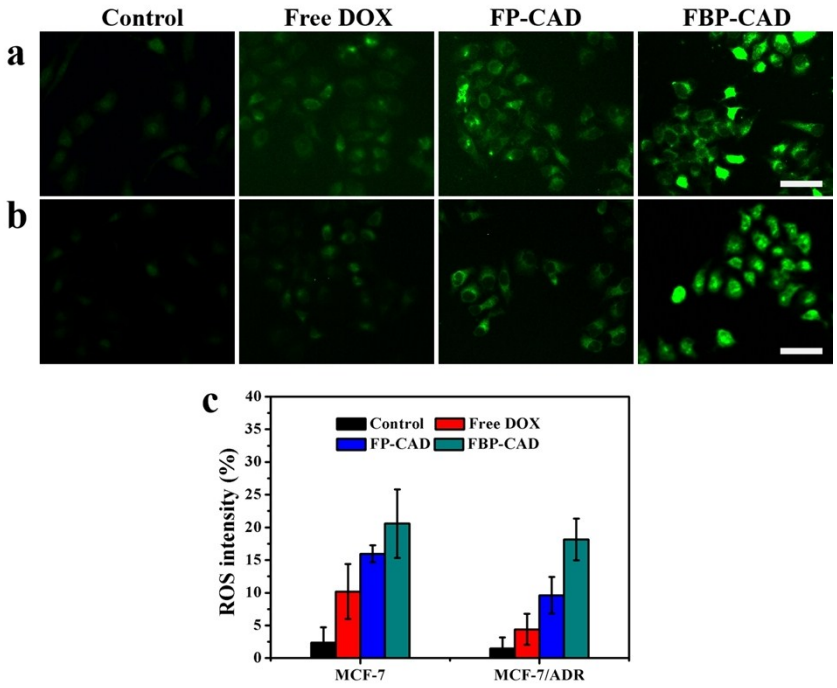

Fig. S15. Intracellular ROS level assessment by DCFH-DA probe in MCF-7 (a) and MCF-7/ADR cells (b), scale bar = 10 μm; Semi-quantitative analysis of ROS fluorescence intensity (c).

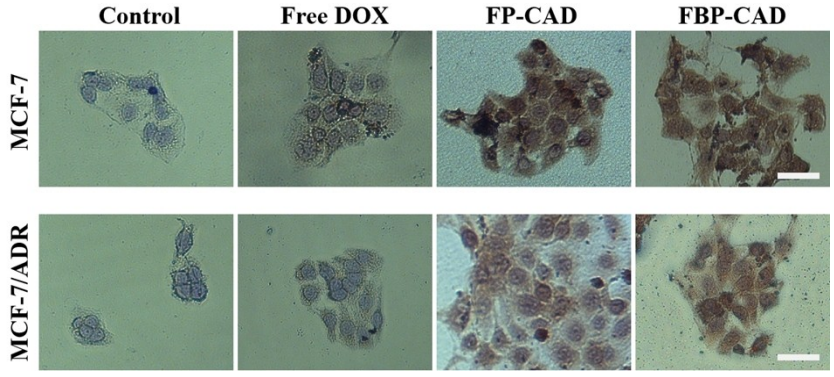

Fig. S16. Cytochrome C (brown colour) release from mitochondrial, scale bar = 10 μm.

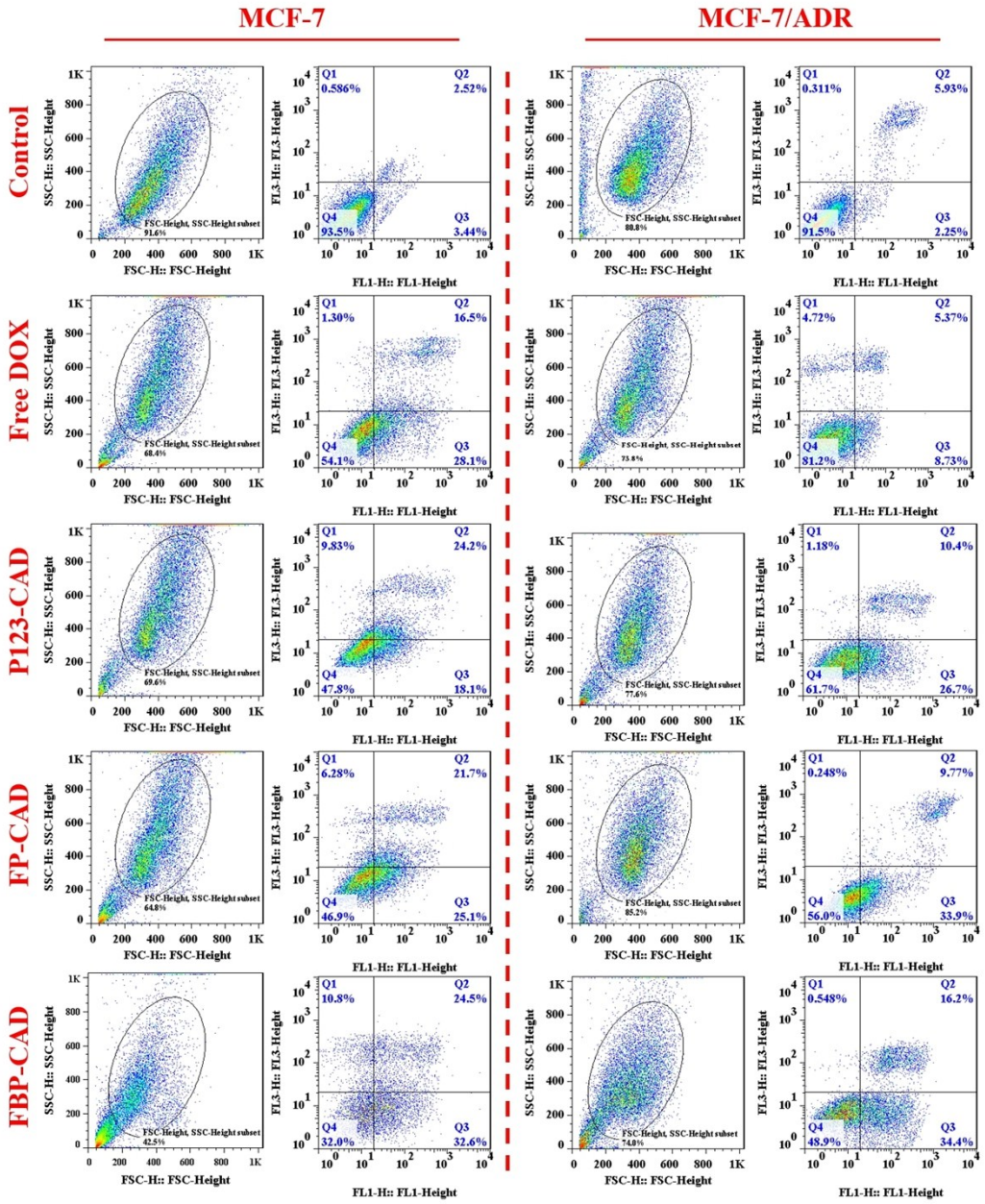

Fig. S17. Cells apoptosis after treatment with free DOX, P123-CAD, FP-CAD and FBP-CAD in MCF-7 (a) and MCF-7/ADR (b) cells.

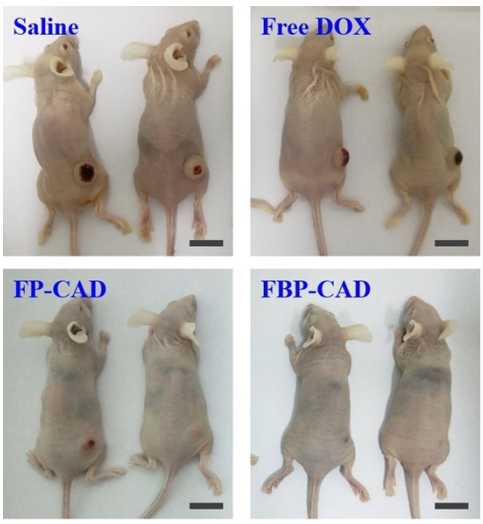

Fig. S18. MCF-7/ADR-bearing mice images after treatment with free DOX, FP-CAD and FBP-CAD for 7 days, scale bar = 2 cm.

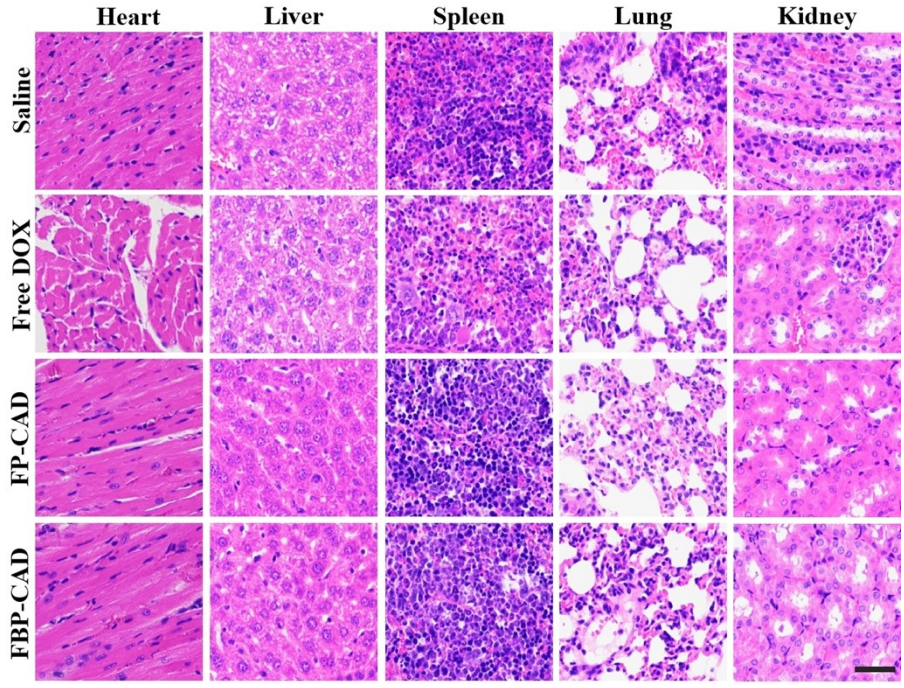

Fig. S19. H&E staining of heart, liver, spleen, lung, kidney, scale bar = 5 μm.

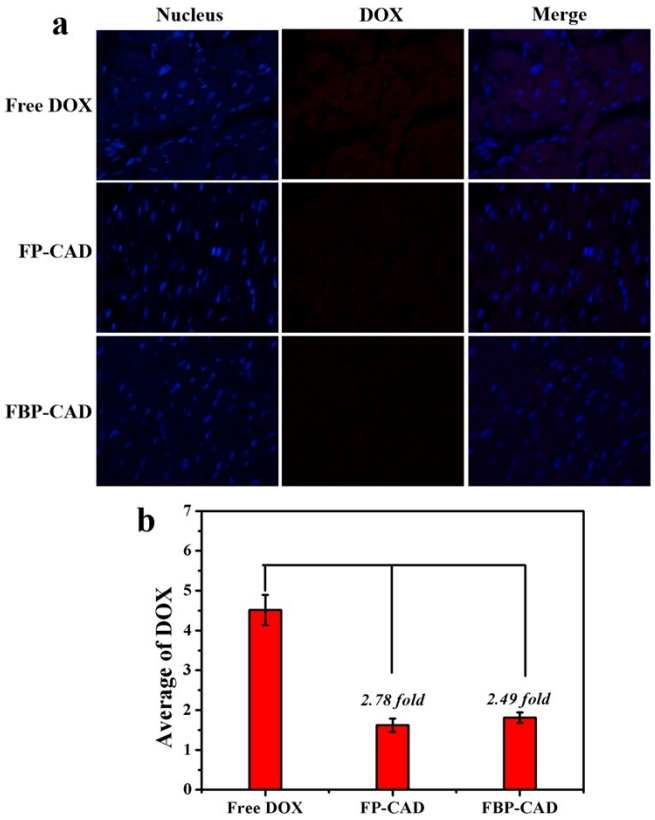

Fig. S20. DOX fluorescence staining in heart tissue after treatment for 24 h (a); Fluorescence intensity statistics (b).

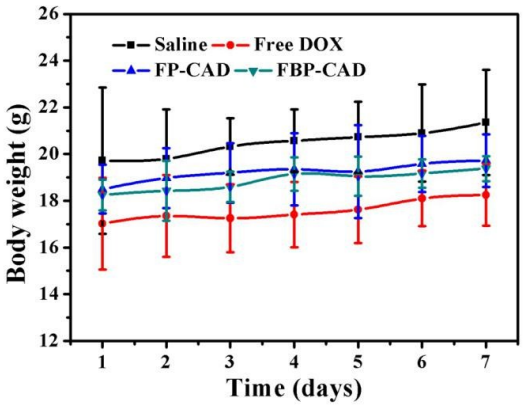

Fig. S21. Mice body change during treatment for 7 days.

Table. S1. IC_{50} value, resistance and reversal index of different formulations against MCF-7 and MCF-7/ADR cells.

Formulations	IC_{50} (μg/mL)		Resistance index	Reversal index
	MCF-7	MCF-7/ADR		
Free DOX	8.34	203.16	24.36	—
FP-DOX	6.12	8.17	1.33	24.87
FBP-DOX	4.5	5.29	1.18	38.4

Resistance index: the ratio of $IC_{50\ (MCF\text{-}7/ADR)}$ against $IC_{50\ (MCF\text{-}7)}$.

Reversal index: the ratio of $IC_{50\ (free\ drug)}$ to $IC_{50\ (drug\text{-}loaded\ micelles)}$ against MCF-7/ADR cells.